上海交通大學
SHANGHAI JIAO TONG UNIVERSITY

Probing the Higgs trilinear self-coupling through Higgs+jet production

Jun Gao, Xiao-Min Shen, Guoxing Wang, Li Lin Yang and **Bin Zhou**

Phys.Rev.D 107 (2023) 11, 115017

The 9th China LHC Physics Workshop, November 17, 2023

Outline

Outline

上海交通大學 SHANGHAI JIAO TONG UNIVERSITY

Experiments[1]

The precise determination of λ_{HHH}

- the electroweak symmetry breaking mechanism
- new physics (NP) beyond the SM

Experiments

- the double-Higgs production: $-0.6 < \kappa_\lambda < 6.6$
- the single-Higgs production: $-4.0 < \kappa_\lambda < 10.3$
- combine them together: $-0.4 < \kappa_\lambda < 6.3$, where $\kappa_\lambda = \lambda_{HHH}/\lambda_{HHH}^{\text{SM}}$.

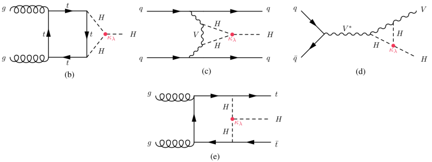

Figure 1: Examples of λ_{HHH}-dependent diagrams for single-Higgs production in the (b) ggF, (c) VBF, (d) VH, and (e) ttH modes.

[1] G. Aad et al. (ATLAS), "Constraints on the Higgs boson self-coupling from single- and double-Higgs production with the ATLAS detector using pp collisions at s=13 TeV", Phys. Lett. B **843**, 137745 (2023).

C-parameter[1]

Consider a beyond-the-SM scenario where the only modification is $\lambda_{HHH}^{\rm SM}$.

$$\lambda_{HHH}^{\rm SM}\, v\, H^3 \to \kappa_\lambda\, \lambda_{HHH}^{\rm SM}\, v\, H^3$$

In the presence of the modified trilinear coupling, a generic NLO observable $\Sigma_{\rm NLO}$ for single Higgs production can be written as

$$\Sigma_{\rm NLO} = Z_H \Sigma_{\rm LO}(1 + \kappa_\lambda C_1)\,, \qquad (1)$$

where C_1 is the process- and kinematic-dependent component. Hence C_1 is different for any production process, a fit involving different measurements can be very powerful for the determination of a single parameter.

[1] G. Degrassi et al., "Probing the Higgs self coupling via single Higgs production at the LHC", JHEP 12, 080 (2016).

C-parameter

上海交通大學 SHANGHAI JIAO TONG UNIVERSITY

In the limit $\kappa_\lambda \to 1$, $Z_H = 1 + \delta Z_H$, and Σ_{NLO} goes to its SM value

$$\Sigma_{\text{NLO}}^{\text{SM}} = \Sigma_{\text{LO}}(1 + C_1 + \delta Z_H)\,, \tag{2}$$

Therefore, C_1 can be extracted as

$$\begin{aligned} C_1 &= \frac{\Sigma_{\text{NLO}}^{\text{SM}} - \Sigma_{\text{LO}} - \delta Z_H \Sigma_{\text{LO}}}{\Sigma_{\text{LO}}} \\ &= \frac{\sum_{i,j} \int dx_1 dx_2 f_i(x_1) f_j(x_2) 2\Re \left(\mathcal{M}^{(0)*}\delta\mathcal{M}_{\text{bare}}^{(1)}\right) d\Phi_2}{\sum_{i,j}\int dx_1 dx_2 f_i(x_1) f_j(x_2)\, |\mathcal{M}^{(0)}|^2 d\Phi_2}, \end{aligned} \tag{3}$$

where the sum goes over all possible partonic initial states i, j; $\delta\mathcal{M}_{\text{bare}}^{(1)}$ don't include contributions coming from the Higgs field renormalization.

Current situations

- All the relevant single Higgs production (ggF, VBF, VH, $t\bar{t}H$, tHj) and decay channels ($\gamma\gamma$, VV^*, $4l$, gg) have been analysed[1,2].
- The calculation of differential effects for ggF is not yet available.
- The analytic expressions of the relevant amplitudes for $pp \to H + jet$ in the large top quark mass expansion up to $O[1/(m_t^2)^3]$ are given in Ref.[3], which are then used to study the effect of κ_λ on the Higgs boson transverse momentum (p_T) distribution[4].

Give reliable predictions in the high energy regions, which are more sensitive to NP beyond the SM!

[1] G. Degrassi et al., "Probing the Higgs self coupling via single Higgs production at the LHC", JHEP **12**, 080 (2016).

[2] F. Maltoni et al., "Trilinear Higgs coupling determination via single-Higgs differential measurements at the LHC", Eur. Phys. J. C **77**, 887 (2017).

[3] M. Gorbahn and U. Haisch, "Two-loop amplitudes for Higgs plus jet production involving a modified trilinear Higgs coupling", JHEP **04**, 062 (2019).

[4] J. Alison et al., "Higgs boson potential at colliders: Status and perspectives", Rev. Phys. **5**, edited by B. Di Micco et al., 100045 (2020).

Outline

Theory Ingredients

Consider four partonic processes

$$g_a(p_1) + g_b(p_2) \to g_c(p_3) + H(p_4),\ q_a(p_1) + \bar{q}_b(p_2) \to g_c(p_3) + H(p_4)$$
$$q_a(p_1) + g_b(p_2) \to q_c(p_3) + H(p_4),\ \bar{q}_a(p_1) + g_b(p_2) \to \bar{q}_c(p_3) + H(p_4)$$

- neglect the masses of all light fermions except that of the top quark
- consider the diagrams including a top-quark loop at LO and both a top-quark loop and a λ_{HHH} vertex at NLO

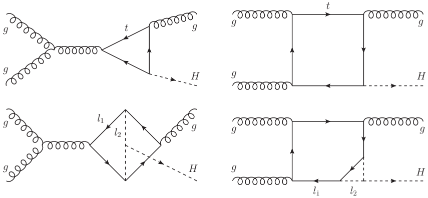

Figure 2: Typical one-loop (upper) and two-loop (lower) Feynman diagrams for the gluon fusion channel.

Amplitude in the gluon fusion channel

The amplitude for the gluon fusion channel is given by

$$\mathcal{M}_{abc}^{gg} = \sqrt[4]{2}\sqrt{G_F}\sqrt{4\pi\alpha_s}\,\mathcal{M}_{abc}^{\mu\nu\rho}\epsilon_\mu(p_1)\epsilon_\nu(p_2)\epsilon_\rho^*(p_3)\,, \tag{4}$$

$\mathcal{M}_{abc}^{\mu\nu\rho}$ can be written as linear combinations of independent tensor structures[1]:

$$\mathcal{M}_{abc}^{\mu\nu\rho} = f_{abc}\sum_{i=1}^{4}\mathcal{T}_{gg,i}^{\mu\nu\rho}A_{gg,i}(\hat{s},\hat{t},m_H,m_t)\,, \tag{5}$$

The form factors can be perturbatively expanded

$$A_{gg,i} = \frac{\alpha_s}{4\pi}\left[A_{gg,i}^{(0)} + \frac{G_F}{2\sqrt{2}\pi^2}A_{gg,i}^{(1)} + \mathcal{O}\left(G_F^2\right)\right]\,, \tag{6}$$

where $A_{gg,i}^{(0)}$ are the one-loop contributions, and $A_{gg,i}^{(1)}$ ($A_{gg,i}^{(1),\mathrm{bare}}$) are the two-loop contributions.

[1] M. Gorbahn and U. Haisch, "Two-loop amplitudes for Higgs plus jet production involving a modified trilinear Higgs coupling", JHEP **04**, 062 (2019).

The large top quark mass expansion up to N^{6}LP

Based on the method of expansion by regions, the integration domain of the loop momenta (l_1, l_2) is divided into four regions: hard-hard, hard-soft, soft-hard and soft-soft.

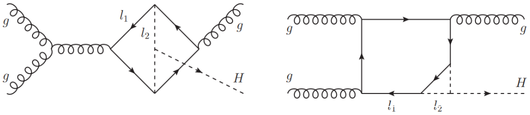

Figure 3: Typica two-loop Feynman diagrams for the gluon fusion channel.

Schematically, we present the $\mathcal{O}[1/(m_t^2)^0]$ (LP) contributions to $A_{gg,i}^{(1),\mathrm{bare}}$ as

$$\vec{A}_{gg}^{(1),\mathrm{bare}} = \frac{m_H^2}{12}\left(-12L_m + 4\sqrt{3}\pi - 23\right)\left(\frac{1}{\hat{t}}, \frac{1}{\hat{s}}, -\frac{1}{\hat{s}}, \frac{1}{\hat{s}} + \frac{1}{\hat{t}} + \frac{1}{\hat{u}}\right), \quad (7)$$

where $L_m = \ln(m_t^2/m_H^2)$. Note that there are no ultraviolet (UV) and infrared (IR) divergences in the form factors.

Padé approximation[1]

A conformal mapping: $w(m_t^2) \equiv \frac{1-\sqrt{1-s'/(4m_t^2)}}{1+\sqrt{1-s'/(4m_t^2)}}$,

The interference with the unexpanded one-loop amplitudes is given by

$$\left[\mathcal{M}^{*(0)}\mathcal{M}^{(j)}\right](w) = \sum_{n=0}^{\infty} b_n^{(j)} w^n \,. \tag{8}$$

The resulting $[m/n]$ Padé approximation for the squared amplitudes takes the following form:

$$\left[\mathcal{M}^{*(0)}\mathcal{M}^{(j)}\right]_{[m/n]} = \frac{c_0^{(j)} + c_1^{(j)} w + \cdots + c_m^{(j)} w^m}{1 + d_1^{(j)} w + \cdots + d_n^{(j)} w^n} \,, \tag{9}$$

In general, there is no way to tell how accurate the approximation is, nor how far the convergent range can be extended.

[1] J. M. Campbell et al., "Two loop correction to interference in $gg \to ZZ$", JHEP **08**, 011 (2016).

Outline

The m_{jh} distributions at LO

Setting:

- $\mu_f = \mu_r = (\sqrt{p_T^2 + m_H^2} + p_T)/2$
- $\sqrt{s} = 13.6\,\text{GeV},\ p_T \geq 20\,\text{GeV}$

where p_T is the transverse momentum of the Higgs boson.

- excellent convergence of the large top quark mass expansion in the region $m_{jh} \leq 2m_t$.
- the relative errors of $[4/2]$ are smaller than 1%.

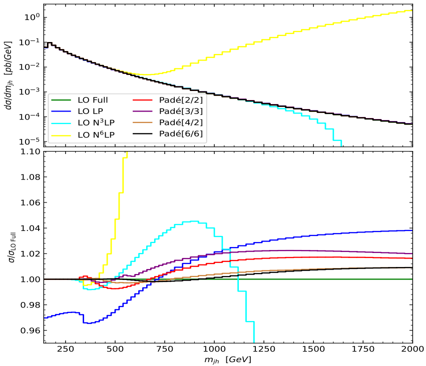

Figure 4: The m_{jh} distributions of $pp \to H + j$ at LO. The lower plot shows the ratios to the LO exact values.

The p_T distributions at LO

Padé approximations

- agreement with the exact results in the small p_T region.
- about 10% relative errors in the large p_T region.
- The Padé approximation works better in the large m_{jh} region than in the large p_T region.

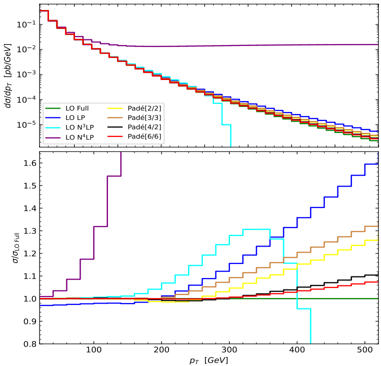

Figure 5: The p_T differential cross sections. The lower plot shows the ratios to the LO exact values.

The total cross sections at LO

上海交通大学 SHANGHAI JIAO TONG UNIVERSITY

Table 1: The LO integrated cross sections (in pb) for $p_T \geq 20\,\mathtt{GeV}$. The error of each number from Monte Carlo integration is given in parentheses.

	σ_{exact}	σ_{LP}	$\sigma_{\text{N}^3\text{LP}}$	$\sigma_{[4/2]}$	$\sigma_{[6/6]}$
LO	13.651(5)	13.304(5)	13.089(5)	13.647(3)	13.652(5)

- The [4/2] and [6/6] Padé approximations show precise estimations of the exact result.

The differential C_1 parameter for m_{jh}

The [4/2] Padé approximation

- agreement with N^{6}LP results in the region $m_{jh} \leq 2m_t$
- C_1 values being around 0.6%
- the small humps near $2m_t$ threshold region

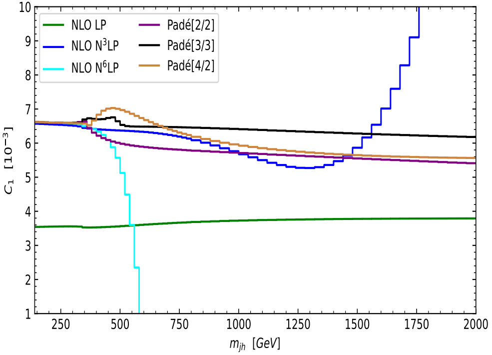

Figure 6: The C_1 parameters with respect to m_{jh}.

The differential C_1 parameter for p_T

上海交通大學 SHANGHAI JIAO TONG UNIVERSITY

The [4/2] Padé approximation

- The deviation from those of the [3/2] and [3/3] approximations are within the relative errors 10%.
- Across the whole range, the values of C_1 is around 0.6%.

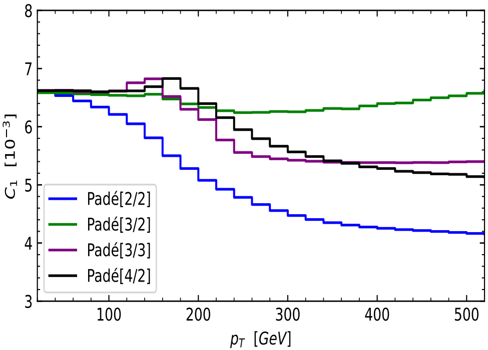

Figure 7: The C_1 parameters with respect to p_T.

The C_1 parameter for total corrections

上海交通大学 SHANGHAI JIAO TONG UNIVERSITY

Table 2: Values of C_1 for total corrections. The relative error of each number from Monte Carlo integration is less than 0.5%.

	C_1^{LP}	$C_1^{\text{N}^3\text{LP}}$	$C_1^{[3/3]}$	$C_1^{[4/2]}$
LO	0.0036	0.0067	0.0066	0.0066

Our best prediction at NLO gives $C_1 = 0.66\%$.

Outline

Summary and Prospects

Summary

- In this work, we give analytic expressions up to $\mathcal{O}[1/(m_t^2)^6]$ (N^{6}LP) for two-loop amplitudes of H+jet with a λ_{HHH} coupling.
- The prediction is then extended to high energy regions by applying the Padé approximation.
- We use the $[4/2]$ Padé approximation as our best prediction at the NLO. We find the values of C_1 at the differential level have a mild dependence on the kinematic variables m_{jh} and p_T, and are around 0.6%. As for the C_1 parameter for total corrections, the value is 0.66%.

Outlook

- Employing more efficient method, for example, the high energy expansion, or the small mass expansion
- Using our results as an additional channel to set extra constraints on λ_{HHH} from the experimental data

Thank you for listening!